Anal. Bioanal. Electrochem., Vol. 14, No. 1, 2022, 45-55

Analytical & Bioanalytical Electrochemistry

2022 by CEE
www.abechem.com

Full Paper

Electrochemical Sensor based on MgO Nanoparticles for Determination of Phenobarbital

Fatemeh Bagrezaei,[1] Ali Fattahi,[1,2,*] and Alireza Khoshroo[3,*]

[1]*Pharmaceutical Sciences Research Center, Health Technology Institute, Kermanshah University of Medical Sciences, Kermanshah, Iran*

[2]*Medical Biology Research Center, Health Institute, Kermanshah University of Medical Sciences, Kermanshah, Iran*

[3]*Nutrition Health Research center, Hamadan University of Medical Sciences, Hamadan, Iran*

*Corresponding Author, Tel.: +989162992291

E-Mails: khoshroo.a.r@gmail.com (A. Khoshroo); a.fatahi.a@gmail.com (A. Fattahi)

Received: 3 January 2021 / Received in revised form: 13 January 2022 / Accepted: 15 January 2022 / Published online: 31 January 2022

Abstract- In this paper, the MgO nanoparticles were used to develop a low-cost carbon paste electrochemical sensor. This sensing platform was used to construct a mediator-free sensor for phenobarbital detection. MgO NPs act as the catalytically active sites for the oxidation of phenobarbital due to their excellent electrochemical properties. The experimental results indicate the excellent catalytic activity of the MgO nanoparticles modified carbon paste electrode (MgO−CE) toward phenobarbital. The cyclic voltammetric results show the significant enhancement of oxidation current (62%) and reduce over-potential oxidation (287 mV) of phenobarbital at the MgO−CE. The improvement of electrochemical signals is due to the accelerated electron transfer between the CE and the phenobarbital. The proposed MgO−CE offers a wide linear range from 1 µM to 1800 µM with a low limit of detection of 0.34 µM and good reproducibility. Given the sensitivity, simplicity, low-cost, accessibility of the materials, it can potentially apply in clinical applications as phenobarbital sensors.

Keywords- Phenobarbital; Ionic liquid; Carbon paste electrode; MgO nanoparticle; Non-enzymatic sensing

1. INTRODUCTION

Phenobarbital (5-ethyl-5-phenylbarturic acid) belongs to the barbiturate family, used as an antiepileptic drug [1]. Phenobarbital is the most common antiepileptic drug and is also used as an antipyretic and analgesic agent to treat various painful symptoms [2]. However, the wide range of side effects and toxicities, e.g., drowsiness, decreased administration, decreased level of consciousness, and shallow breathing, together with difficulty in controlling epilepsy symptoms, made the continuous monitoring of phenobarbital crucial [3–5]. Therefore, it is necessary to design simple, cheap, fast, and reliable protocols that can quickly determine phenobarbital in the serum samples. Although various analytical methods, e.g., optical biosensors [6], capillary electrophoresis [7], gas chromatography [8], and liquid chromatography [9] have already been proposed to determine the phenobarbital in biological samples and pharmaceutical formulations; they are complex and need expensive equipment. Accordingly, electrochemical methods have the advantages of simplicity, low toxicity of reagents, relatively low cost, reliability, and low detection limit compared to other analytical techniques, therefore, these methods are widely applied for the analysis of food and pharmaceuticals analytes [10–18]. The development of electrochemical sensors based on modified electrodes has been considered because they can cover a wide range of economic and straightforward analyzes. Also, one of the most attractive fields in electrochemistry is the development of susceptible and selective methods based on nanomaterials. Recently, various nanomaterials such as metal nitride nanoparticles, metal oxide nanoparticles, noble metal nanoparticles, and carbon-based nanomaterials have been used to increase the analytical performance of biosensors [19–21]. Among these materials, nanostructured metal oxides, with smaller crystal sizes and high surface area, have applications such as optical, measuring devices, and electronics [22–25]. Today, metal oxide nanoparticles are used in various shapes, sizes, and combinations to measure electroactive materials. According to scientific research, nanomaterials can not only reduce the charge transfer resistance of electrodes but also increase the sensitivity of modified sensors. So far, various metal oxide nanostructures such as TiO_2, MgO, Fe_3O_4, ZnO, and $CoFe_2O_4$ have been synthesized for various applications [26–28]. Among these metal oxide nanostructures, the MgO nanostructure finds wide applications in multiple fields due to its unique nature [29,30]. Based on these properties, MgO nanostructure was used in a wide range of applications such as antibacterial agents [31], gas separation performance membranes [32], dye removal agents [33], electro-catalyst [34]. Despite the wide range of applications of MgO nanostructure in various fields, a few works are reported on the electrochemical activity of MgO nanostructure [34-36].

In this study, for the first time, MgO nanoparticles were used for the construction of a modified carbon paste electrode for the determination of phenobarbital. The MgO nanoparticles were synthesized via the sol-gel process and characterized using Fourier-transform infrared spectroscopy (FTIR), scanning electron microscopy (SEM), transmission

electron microscopy (TEM), energy dispersive X-Ray (EDX), and X-ray diffraction (XRD). MgO NPs show good electrocatalytic activity toward oxidation of phenobarbital. Therefore, based on the electrocatalytic response of the electrode, the sensitive determination of phenobarbital could be achieved.

2. EXPERIMENTAL SECTION

2.1. Apparatus and chemicals

Oxalic acid ($(COOH)_2.2H_2O$), magnesium acetate tetrahydrate ($Mg(CH_3COO)_2.4H_2O$), 1-butyl-3-methylimidazolium hexafluorophosphate ($[BMIM]PF_6$), and $K_4[Fe(CN)_6]$ were purchased from Sigma Aldrich. Graphite powder, paraffin, ethanol, and acetone were purchased from Merck company. All the chemical reagents were used without any purification. All aqueous solutions were prepared in distilled water**.**

The electrochemical analysis was carried out with Autolab potentiostat/galvanostat (PGSTAT101) to evaluate the catalytic effect of the MgO modified electrode. XRD analysis was performed on the Bruker AXSD8 Advance diffractometer operating in the reflection mode with Cu-Kα radiation (40 kV, 30 mA) in the range of 5-80°. The magnesium oxide nanoparticles' morphological study was conducted by the HIT-4160-02 scanning electron microscope (SEM). Also, the morphology, size, and shape of the synthesized nanoparticles were examined by a transmission electron microscope (Zeiss EM 900) with an accelerating voltage of 200 kV. The results of the EDX analysis were performed by a ZEISS Ultra-55 device. The FTIR of MgO was performed by IR-Prestige-21 (SHIMADZU Spectrometer, Kyoto, Japan); KBr Pellets of samples were used to measure transmittance percentage.

2.2. Synthesis of MgO nanoparticles

For the preparation of MgO nanoparticles via the sol-gel process, the equimolar ratio of magnesium acetate and oxalic acid was added to absolute ethanol. The resulting clear solutions were then mixed and stirred vigorously for 30 min to give a white gel. The obtained white gel was stirred at room temperature for 12 h to digest. After that, it was placed in an oven at 100 °C for drying. Finally, the achieved white powder was calcined at 600 °C to give magnesium oxide nanoparticles [37].

2.3. Preparation of the electrode

The modified electrodes were prepared by dispersion of 0.01 g magnesium oxide nanoparticles in 2 mL ethanol and were added in 1.0 g of graphite. Then, 0.05 mL $[BMIM]PF_6$ and 0.15 mL of paraffin were added to the above mixture and mixed until a homogeneous wet dough was obtained. Finally, the end of a glass tube was filled with paste, and electrical contact was produced by placing a copper wire inside the modified MgO carbon paste (MgO−CE). The

bare carbon paste electrodes (CE) were fabricated by the same method but in the absence of MgO nanoparticles with the mentioned formulation. Then, polishing the electrode surface was done by hand polishing on the sheet of paper (this eliminates the excess amount of paraffin). By pushing and guiding the past out of the rod and polishing it by hand on white filter paper, a new surface is created on the electrode.

3. RESULTS AND DISCUSSION

3.1. Characterization of MgO nanoparticles

The MgO nanoparticles were characterized by FT-IR, XRD, SEM, EDX, and TEM. According to the FT-IR spectrum (Fig. 1a), the absorption band at 3461cm^{-1} is attributed to the O–H stretching frequency of O-H groups attached to the surface of MgO nanoparticles. The Mg-O stretching peak appears at 1381 cm^{-1}. The peak appearing in 548 cm^{-1} is related to the stretching vibration of Mg-O [38]. The crystalline nature of magnesium oxide nanoparticles was determined by the XRD technique and the X-ray pattern of the synthesized magnesium oxide nanoparticles is illustrated in Fig. 1b. The peaks at 2θ values of 36.92, 42.97, 62.37, 74.97, and 78.82 with miller coefficients of (111), (200), (220), (311), and (222) confirmed the Face Centered Cubic (FCC) lattice structure of MgO NPs with a space group of Fm-3m (JCPDS file no. 89-7746). The absence of additional peaks in the XRD spectrum confirms the synthesis of MgO nanoparticles with very high purity [38].

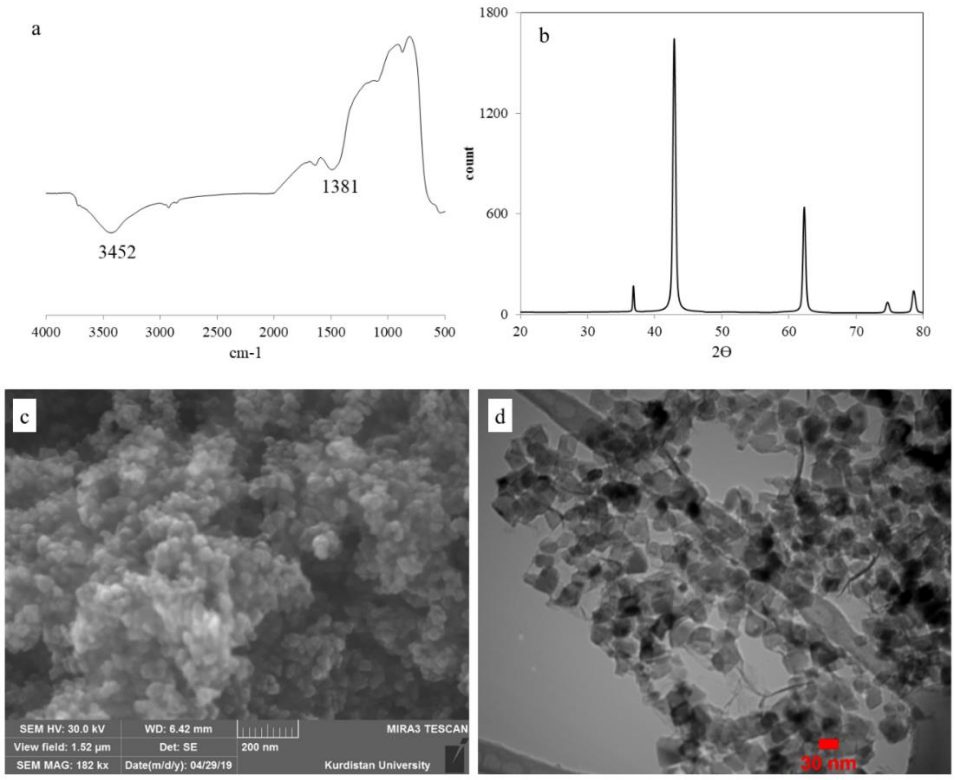

Figure 1. a) FT-IR spectrum, b) XRD pattern, c) SEM image, and d) TEM image

The morphology of MgO NPs was investigated by SEM and according to Fig. 1c, the average particle size is between 15-20 nm. TEM is another technique used to study the shape and size of nanoparticles. According to the TEM image (Fig. 1d), MgO NPs have a cubic structure and are evenly dispersed. Also, based on the particle distribution histogram (Fig. S1), particles with a size of 10-20 nm have the highest number statistically and also SEM results are in good agreement with TEM results.

EDX is a useful technique to determine the elements and the percentage of their distribution at the nanoparticle surface. Fig. S2 illustrated the EDX pattern of MgO NPs. It confirmed that the as-synthesized material is made of magnesium and oxygen. Thus, the pure MgO NPs were synthesized successfully.

3.2. Electrochemical characterization of MgO modified electrode

Cyclic voltammetry with a range of −200 to 700 mV was used to investigate the electrochemical performance of MgO modified carbon paste electrodes. Fig. 2a shows the cyclic voltammogram at the CE and MgO−CE in the presence of $[Fe(CN)_6]^{4-/3-}$ at the scan rate of 100 mV s^{-1}. As can be seen, a pair of redox peaks are observed at the bare and modified electrode with MgO NPs. After the modification of bare CE with MgO NPs, the peak current increased clearly (MgO−CE), which was attributed to the high active surface area of the CE modified with MgO NPs. The CE and MgO−CE electrodes were investigated using cyclic voltammetry at various scan rates (from 10 to 500 mV s^{-1}) to determine their active surface areas (Fig. 2b and Fig. S3). The Randles–Sevcik Equation was used to estimate the active surface area based on the plots of peak currents *vs.* scan rate$^{1/2}$ for the CE and MgO−CE electrodes in 1.0 mM $[Fe(CN)_6]^{4-/3-}$ (Fig. 2c). The active surface area was 0.17 and 0.21 cm^2 for CE and MgO−CE electrodes, respectively. The results indicated that the electrode effective surface area in the presence of MgO NPs was increased by about ~20%, which can enhance the sensitivity of CE electrodes in the presence of MgO NPs.

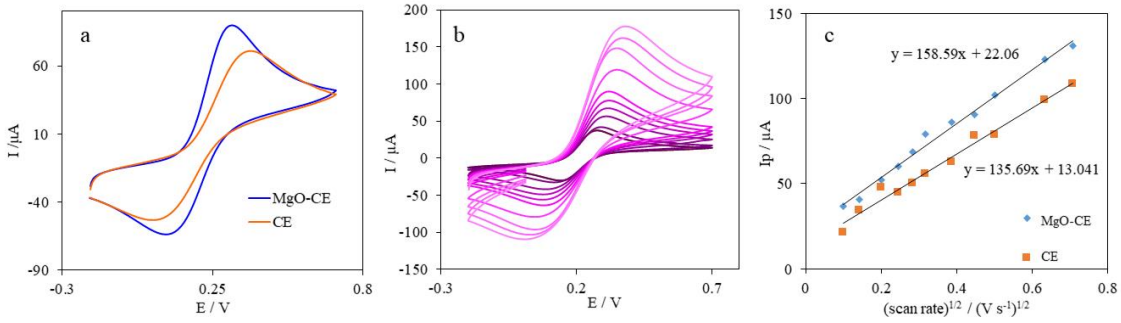

Figure 2. (a) CVs of CE and MgO-CE in the 1.0 mM $[Fe(CN)_6]^{3-/4-}$, (b) CVs of MgO-CE in 1.0 mM $[Fe(CN)_6]^{3-/4-}$ at different scan rates, from 10 to 500 mV s^{-1}, (c) Variation of I_p *vs.* $v^{1/2}$ for CE and MgO-CE

3.3. Electrocatalytic properties of MgO−CE electrodes for phenobarbital

To investigate the electrochemical performance of MgO NPs towards phenobarbital oxidation, cyclic voltammograms of phenobarbital at the CE, and MgO−CE electrodes at the scan rate of 100 mV s^{-1} were performed. As can be seen, the oxidation current of phenobarbital was increased in the presence of MgO NPs (MgO−CE). The comparison of oxidation peaks current of phenobarbital at the MgO−CE and CE (Fig. 3b) confirms that the oxidation current increased 1.62 times (62%) and over-potential reduce 287 mV in the presence of MgO NPs.

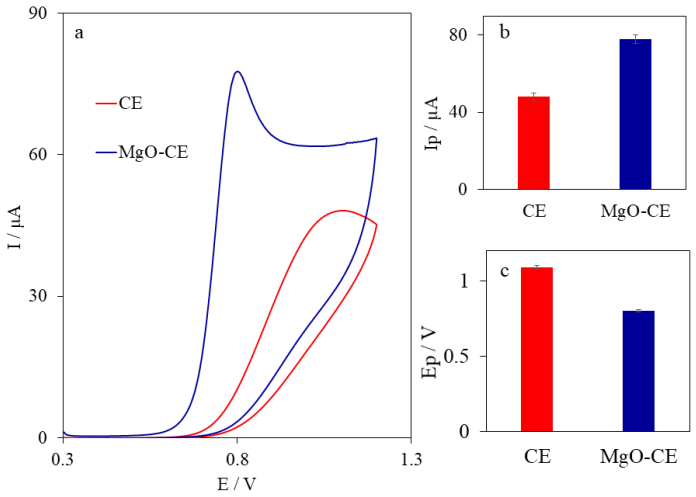

Figure 3. (a) CVs of CE and MgO-CE in the presence of 1.2 mM phenobarbital in 0.1 M phosphate buffer solution (pH 7.0) at a scan rate of 100 mV s^{-1}. The peak currents (b) and peak potential (c) for 1.2 mM phenobarbital at the CE and MgO-CE electrodes

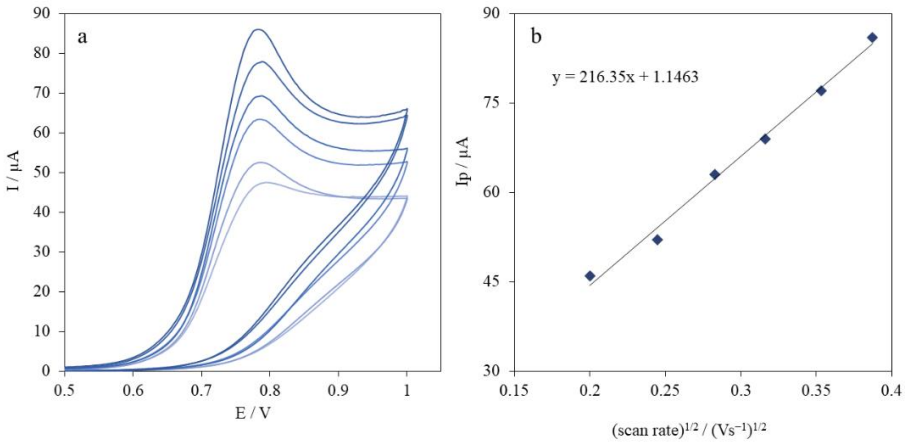

Figure 4. (a) CVs of MgO-CE in 0.1 M phosphate buffer solution (pH 7.0) containing 1.0 mM phenobarbital at various scan rates, from 40 to 150 mV s^{-1}, (b) Variation of peak current *vs.* $v^{1/2}$

The effect of scan rate on the oxidation of phenobarbital at the MgO−CE was investigated by CV at the different scan rates from 40 to 150 mV^{-1} (Fig. 4). The oxidation peak currents of phenobarbital at the MgO−CE increased with increasing scan rate, which is a linear dependence between the currents and $\nu^{1/2}$. This dependence was described with $I(\mu A)=1.14+216.3(\nu)^{1/2}$, which illustrates the diffusion-controlled process of phenobarbital on the MgO−CE.

3.4. Calibration curve of phenobarbital at MgO−CE

Differential pulse voltammetry (DPV) was used for the determination of the linear range and limit of detection of phenobarbital at the MgO−CE in the presence of various phenobarbital concentrations. Fig. 4 shows the DPV curve of various concentrations of phenobarbital at MgO−CE. The DPV current related to the phenobarbital oxidation at the MgO−CE increased with phenobarbital concentration. The calibration plot of phenobarbital *vs.* DPV peak currents is shown in the inset of Fig. 4, which consists of two linear parts; an equation of $I_p(\mu A)=0.0174\ C_{phenobarbital}+0.121$ for the first part (1.0–400 µM) and an equation of $I_p(\mu A)=0.0083\ C_{phenobarbital}+4.023$ for the second linear part (400–1800 µM). The limit of detection for the detection of phenobarbital by MgO−CE was calculated as 0.34 µM from the slop of the calibration plot ($3s_b$/slope). The recommended therapeutic dosage of phenobarbital is 15–40 mg/L (64−172 µM) [39]. The results confirm the potential applications of the MgO−CE in real samples. Table 1 compares the analytical performance of the MgO−CE with some sensors for phenobarbital. The MgO−CE provides a sensitive technique for the determination of phenobarbital.

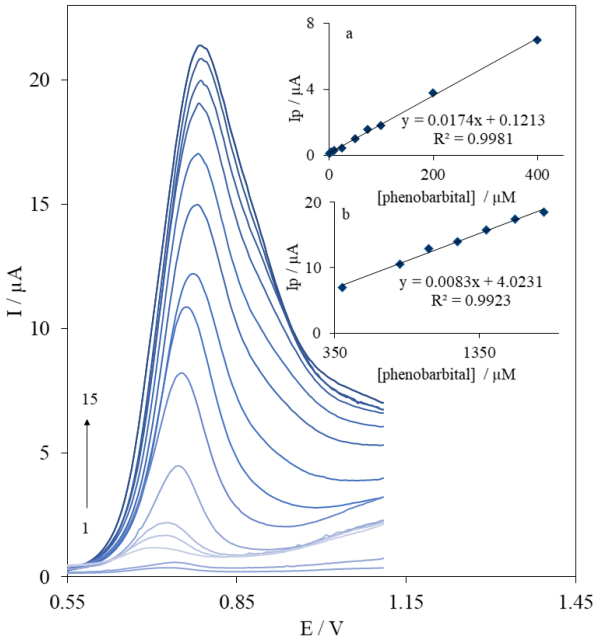

Figure 5. DPVs of MgO-CE in different concentrations of phenobarbital, numbers 1-15 correspond to 1.0-1800 µM, Plot of the peak currents as a function of phenobarbital concentration in the range of (a) 1.0-400 µM (b) 400-1800 µM

To the examination of MgO−CE for practical applications, the prepared electrode with MgO NPs was used with the measurements of phenobarbital in serum samples. The 0.5 mL serum samples were mixed with 9.5 mL of PBS, and the response was achieved by peak current which was obtained from DPV. As shown in Table 2, the obtained phenobarbital contents in serum samples by MgO−CE are in good agreement with the spiked amount of phenobarbital on the samples. The recovery calculated by MgO−CE was in the range of 96.8% to 102.7%. These results show that the MgO−CE can be applied for the determination of phenobarbital in real samples.

Table 1. A comparison of the performance of several sensors for the detection of phenobarbital

Electrode materials	Linear range (μM)	The detection limit (μM)	Ref.
Multi-walled carbon nanotube and Pt-nanoparticles	0.4-60	0.1	[40]
Ni nanoparticle	0.14-1300	0.008	[41]
Molecularly imprinted polymer based on methacrylic acid	0.9-50	0.5	[42]
CuO nanoparticle-modified molecularly imprinted	0.01-180	0.0023	[43]
Gold Electrode	1.0-35	0.19	[44]
MgO-CPE	1.0-1800	0.34	This work

Table 2. Determination and recovery results of phenobarbital in the human serum samples by MgO-CE

Sample	Added (μM)	Found (μM)	Recovery (%)
Serum	-	<DL	-
	50	48.4	96.8
	100	99.8	99.8
	150	153.9	102.6
	200	205.4	102.7

3.5. The repeatability and interference study of MgO−CE

The reproducibility of MgO−CE was investigated with the electrochemical response of 100 μM phenobarbital by DPV at the four MgO−CE electrodes which was constructed with the same method. The RSD for DVP response was 2.9%., which indicated that the MgO−CE showed good reproducibility toward phenobarbital determination. Moreover, the RSD of the

four measurements of 100 μM phenobarbital for single MgO−CE was 2.1%, indicating acceptable reproducibility.

Also, the effect of various foreign species on the electrochemical response of MgO−CE toward phenobarbital was investigated. A 50-fold concentration of Na^+, Mg^{2+}, Cu^{2+}, K^+, Cl^-, Fe^{2+}, NO_3^-, and a 20-fold concentration of urea, phenylalanine, ethanol, proline, methanol, fructose and glucose was added to a 1.0 mM phenobarbital. Then, the MgO−CE was applied for the determination of phenobarbital in this mixture. Based on the obtained results, no relative signal change over ±5% was observed, which suggests that the presence of the mentioned interfering species does not affect the MgO−CE responses toward phenobarbital detection.

4. CONCLUSION

A simple and low-cost sensor based on MgO NPs was developed for the determination of phenobarbital. The MgO NPs were prepared by the simple sol-gel process. The MgO NPs with excellent electrocatalytic properties were used in developing a carbon paste sensor for the determination of phenobarbital. The proposed sensor is simple and does not need any high-cost materials or complicated fabrication processes. The modified electrode with MgO NPs exhibits a good catalytic response toward phenobarbital, with a linear range of 1 – 1800 μM and limit of detection (LOD) of 0.34 μM (S/N = 3).

Acknowledgments

The authors gratefully acknowledge the Research Council of Kermanshah University of Medical Sciences for supports. This work was performed in partial fulfilment of the requirements for Pharm. D of Fatemeh Bagrezaei, in Faculty of Pharmacy, Kermanshah University of Medical Sciences, Kermanshah, Iran.

Authors contributions

Fatemeh Bagrezaei: Methodology, Investigation, Writing - Original Draft
Alireza Khoshroo: Conceptualization, Investigation, Writing - Review & Editing
Ali Fattahi: Conceptualization, Funding acquisition, Writing - Review & Editing

Conflicts of interest/Competing interests

The authors declare that they have no competing interests.

REFERENCES

[1] S. I. Johannessen, and C. Johannessen Landmark, Neuro-Psychopharmacotherapy (2020) 1.
[2] C. M. Monzón, M. del C. Sarno, and M. R. Delfino, Sci-ELO Argentina (2008) 101.

[3] R. Shariati, B. Rezaei, H. R. Jamei, and A. A. Ensafi, Talanta 194 (2019) 143.
[4] V. Spiehler, L. Sun, D. S. Miyada, S. G. Sarandis, E. R. Walwick, M. W. Klein, D. B. Jordan, and B. Jessen, Clin. Chem. 22 (1976) 749.
[5] Z. Es'haghi, Z. Rezaeifar, G. -H. Rounaghi, Z. A. Nezhadi, and M. A. Golsefidi, Anal. Chim. Acta 689 (2011) 122.
[6] V. Garzón, D. G. Pinacho, R. -H. Bustos, G. Garzón, and S. Bustamante, Biosensors 9 (2019) 132.
[7] A. Haque, X. Xu, and J. T. Stewart, J. Pharm. Biomed. Anal. 21 (1999) 1063.
[8] H. J. Kupferberg, Clin. Chim. Acta 29 (1970) 283.
[9] A. Serralheiro, G. Alves, A. Fortuna, M. Rocha, and A. Falcão, J. Chromatogr. B 925 (2013) 1.
[10] L. Hosseinzadeh, A. Khoshroo, K. Adib, M. Rahimi-Nasrabadi, and F. Ahmadi, Microchem. J. 165 (2021) 106124.
[11] A. Sobhani-Nasab, S. M. Hoseinpour, M. Rahimi-Nasrabadi, S. Pourmasoud, M. Eghbali-Arani, and F. Ahmadi, J. Mater. Sci. Mater. Electron. 32 (2021) 26998.
[12] M. Hafezi, M. Rostami, A. Hosseini, M. Rahimi-Nasrabadi, M. Fasihi-Ramandi, A. Badiei, and F. Ahmadi, J. Mol. Liq. 322 (2021) 114875.
[13] M. Rostami, A. S. Nasab, M. Fasihi-Ramandi, A. Badiei, M. Rahimi-Nasrabadi, and F. Ahmadi, New J. Chem. 45 (2021) 4280.
[14] E. Sohouli, M. Ghalkhani, T. Zargar, Y. Joseph, M. Rahimi-Nasrabadi, F. Ahmadi, M. E. Plonska-Brzezinska, and H. Ehrlich, Electrochim. Acta (2021) 139633.
[15] M. H. Ghanbari, A. Khoshroo, H. Sobati, M. R. Ganjali, M. Rahimi-Nasrabadi, and F. Ahmadi, Microchem. J. 147 (2019) 198.
[16] A. Khoshroo, K. Sadrjavadi, M. Taran, and A. Fattahi, Sens. Actuators B 325 (2020) 128778.
[17] M. Mazloum-Ardakani, E. Amin-Sadrabadi, and A. Khoshroo, J Electroanal Chem 775 (2016) 116.
[18] A. Khoshroo, L. Hosseinzadeh, K. Adib, M. Rahimi-Nasrabadi, and F. Ahmadi, Anal. Chim. Acta 1146 (2021) 1.
[19] M. Mazloum-Ardakani, F. Sabaghian, A. Khoshroo, and H. Naeimi, Chinese J. Catal. 35 (2014) 565.
[20] M. Mazloum-Ardakani, V. Eslami, and A. Khoshroo, Mater. Sci. Eng. B 229 (2018) 201.
[21] M. Mehmandoust, N. Erk, O. Karaman, F. Karimi, M. Bijad, and C. Karaman, Food Chem. Toxicol. 158 (2021) 112698.
[22] M. Rahimi-Nasrabadi, F. Ahmadi, and M. Eghbali-Arani, J. Mater. Sci. Mater. Electron. 28 (2017) 2415.
[23] A. Lempicki, Proc Phys. Soc. 66 (1953) 281.

[24] M. Rahimi-Nasrabadi, F. Ahmadi, and M. Eghbali-Arani, J. Mater. Sci. Mater. Electron. 27 (2016) 13294.
[25] M. Rahimi-Nasrabadi, S. M. Pourmortazavi, M. Aghazadeh, M. R. Ganjali, M. S. Karimi, and P. Norouzi, J. Mater. Sci. Mater. Electron. 28 (2017) 9478.
[26] B. Zhang, and P. X. Gao, Front. Mater. 6 (2019) 55.
[27] S. Sagadevan, S. Vennila, J. A. Lett, A. R. Marlinda, N. A. B. Hamizi, and M. R. Johan, Results Phys. 15 (2019) 102543.
[28] M. Mazloum-Ardakani, and A. Khoshroo, Phys. Chem. Chem. Phys. 17 (2015) 22985.
[29] A. A. Pilarska, Ł. Klapiszewski, and T. Jesionowski, Powder Technol. 319 (2017) 373.
[30] Z. X. Tang, and B. F. Lv, Brazilian J. Chem. Eng. 31 (2014) 591.
[31] T. Jin, and Y. He, J. Nanoparticle Res. 13 (2011) 6877.
[32] S. S. Hosseini, Y. Li, T. S. Chung, and Y. Liu, J Memb Sci 302 (2007) 207.
[33] G. Moussavi, and M. Mahmoudi, J. Hazard. Mater. 168 (2009) 806.
[34] L. S. R. Yadav, K. Lingaraju, K. Manjunath, G. K. Raghu, K. H. S. Kumar, and G. Nagaraju, Mater. Res. Express 4 (2017) 25028.
[35] V. Arabali, and H. Karimi-Maleh, Anal. Methods 8 (2016) 5604.
[36] M. Li, W. Guo, H. Li, W. Dai, and B. Yang, Sens. Actuators B 204 (2014) 629.
[37] M. S. Mastuli, N. Kamarulzaman, M. A. Nawawi, A. M. Mahat, R. Rusdi, and N. Kamarudin, Nanoscale Res. Lett. 9 (2014) 134.
[38] J. P. Dhal, M. Sethi, B. G. Mishra, and G. Hota, Mater. Lett. 141 (2015) 267.
[39] J. Methaneethorn, D. Panomvana, and T. Vachirayonstien, Drug Metab. Pers. Ther. 32 (2017) 151.
[40] J. B. Raoof, M. Baghayeri, and R. Ojani, Colloids Surfaces B 95 (2012) 121.
[41] H. C. Yu, X. Y. Huang, F. H. Lei, X. C. Tan, Y. C. Wei, and H. Li, Electrochim. Acta 141 (2014) 45.
[42] H. Quan, S. -U. Park, and J. Park, Electrochim. Acta 55 (2010) 2232.
[43] H. C. Yu, X. Y. Huang, H. Li, F. H. Lei, X. C. Tan, Y. C. Wei, and H. Y. Wu, Acta Physico-Chimica Sinica 30 (2014) 2085.
[44] M. A. Ivić, J. Antanasijević, N. Trišović, D. Antanasijević, J. Lović, D. Mijin, and S. Petrović, Int. J. Electrochem. Sci. 11 (2016) 5935.